Unclassified
SECURITY CLASSIFICATION OF THIS PAGE

(4)

REPORT DOCUMENTATION PAGE

AD-A199 574

1b. RESTRICTIVE MARKINGS

3. DISTRIBUTION/AVAILABILITY OF REPORT
Approved for public release;
Distribution unlimited

4. PERFORMING ORGANIZATION REPORT NUMBER(S)
AFGL-TR-88-0207

5. MONITORING ORGANIZATION REPORT NUMBER(S)

DTIC
ELECTE
SEP 16 1988
D

6a. NAME OF PERFORMING ORGANIZATION	6b. OFFICE SYMBOL (If applicable)	7a. NAME OF MONITORING ORGANIZATION
Air Force Geophysics Laboratory		

6c. ADDRESS (City, State, and ZIP Code)	7b. ADDRESS (City, State, and ZIP Code)
Hanscom AFB Massachusetts 01731-5000	

8a. NAME OF FUNDING/SPONSORING ORGANIZATION	8b. OFFICE SYMBOL (If applicable)	9. PROCUREMENT INSTRUMENT IDENTIFICATION NUMBER

8c. ADDRESS (City, State, and ZIP Code)	10. SOURCE OF FUNDING NUMBERS			
	PROGRAM ELEMENT NO.	PROJECT NO.	TASK NO.	WORK UNIT ACCESSION NO.
	62101F	6670	17	07

11. TITLE (Include Security Classification)
Color-Composite Image Processing for Multispectral Meteorological Satellite Data

12. PERSONAL AUTHOR(S)
Robert d'Entremont, Larry W. Thomason, James Bunting

13a. TYPE OF REPORT	13b. TIME COVERED	14. DATE OF REPORT (Year, Month, Day)	15. PAGE COUNT
REPRINT	FROM _____ TO _____	1988 September 12	11

16. SUPPLEMENTARY NOTATION
Reprinted from Proceedings of the SPIE, Vol 846, pp 96-106, Oct 1987

17. COSATI CODES			18. SUBJECT TERMS (Continue on reverse if necessary and identify by block number)
FIELD	GROUP	SUB-GROUP	Multispectral satellite imagery; Cloud analysis; Multispectral data; Image Processing

19. ABSTRACT (Continue on reverse if necessary and identify by block number)

Visible and infrared satellite imagery data are a primary source of global cloud observations. Visible channels measure reflected solar energy and are used to detect clouds and snow. Infrared channels measure emitted thermal energy, and, consequently, the brightness temperatures of clouds and the earth's surface both day and night. It is sometimes difficult to interpret such imagery because of varying conditions encountered on global scales. Snow cover is often confused with clouds in visible imagery because each surface reflects sunlight well. Low clouds are frequently confused with cloudfree land and oceans in infrared imagery because their temperatures can be nearly equal. It is found that more confident discriminations can be performed between such features when DMSP Operational Linescan System (OLS), NOAA Advanced Very High Resolution Radiometer (AVHRR), or Nimbus Scanning Multifrequency Microwave Radiometer (SMMR) data are combined into color image products. A multispectral image display technique is described that simultaneously combines several meteorological satellite images into a color image product. The technique, which has its origin in Landsat Multispectral Scanner image processing, is quick & effective, & clearly reveals many (OVER)

20. DISTRIBUTION/AVAILABILITY OF ABSTRACT	21. ABSTRACT SECURITY CLASSIFICATION
☐ UNCLASSIFIED/UNLIMITED ☒ SAME AS RPT ☐ DTIC USERS	Unclassified

22a. NAME OF RESPONSIBLE INDIVIDUAL	22b. TELEPHONE (Include Area Code)	22c. OFFICE SYMBOL
James Bunting		AFGL/LYS

DD FORM 1473, 84 MAR

83 APR edition may be used until exhausted.
All other editions are obsolete.

SECURITY CLASSIFICATION OF THIS PAGE
Unclassified

CONT OF BLOCK 19:

features of meteorological interest.

AFGL-TR-88-0

A Reprint from the

PROCEEDINGS

Of SPIE-The International Society for Optical Engineering

Volume 846

Digital Image Processing and Visual Communications Technologies in Meteorology

27-28 October 1987
Cambridge, Massachusetts

Color-composite image processing for multispectral meteorological satellite data

Robert P. d'Entremont, Larry W. Thomason, James T. Bunting
Satellite Meteorology Branch, Atmospheric Sciences Division
U.S. Air Force Geophysics Laboratory, Hanscom AFB, MA 01731-5000

Accession For
NTIS GRA&I [X]
DTIC TAB [ ]
Unannounced [ ]
Justification
By
Distribution/
Availability Codes
Dist | Avail and/or Special
A-1 | 20

color
reproduct-
will be in black and

©1987 by the Society of Photo-Optical Instrumentation Engineers
Box 10, Bellingham, Washington 98227 USA Telephone 206 676-3290

88 9 16 211

Color-composite Image Processing For Multispectral Meteorological Satellite Data

Robert P. d'Entremont, Larry W. Thomason, and James T. Bunting

Satellite Meteorology Branch, Atmospheric Sciences Division
Air Force Geophysics Laboratory
Hanscom A.F.B., MA 01731-5000

Abstract

Visible and infrared satellite imagery data are a primary source of global cloud observations. Visible channels measure reflected solar energy and are used to detect clouds and snow. Infrared channels measure emitted thermal energy and, consequently, the brightness temperatures of clouds and the earth's surface both day and night. It is sometimes difficult to interpret such imagery because of varying conditions encountered on global scales. Snow cover is often confused with clouds in visible imagery because each surface reflects sunlight well. Low clouds are frequently confused with cloudfree land and oceans in infrared imagery because their temperatures can be nearly equal. It is found that more confident discriminations can be performed between such features when DMSP Operational Linescan System (OLS), NOAA Advanced Very High Resolution Radiometer (AVHRR), or Nimbus Scanning Multifrequency Microwave Radiometer (SMMR) data are combined into color image products. A multispectral image display technique is described that simultaneously combines several meteorological satellite images into a color image product. The technique, which has its origin in Landsat Multispectral Scanner image processing, is quick and effective, and clearly reveals many features of meteorological interest.

Keywords: Multispectral Satellite Imagery, Multispectral Data, Image Processing, Cloud Analysis.

1. Introduction

Most of the satellite imagery used by meteorologists comes from "visible" and "infrared" window channels (0.4-0.7μm and 10-12μm, respectively). Visible imagery is used in the daytime to detect clouds or surface features; infrared imagery is used both day and night and provides for the analysis of cloud-top and surface skin temperatures.

There are limitations to the effectiveness of visible and infrared imagery. Visible data is useful for detecting clouds since usually they reflect sunlight more strongly than most backgrounds. However, cloudfree snow and ice can reflect sunlight just as well as clouds, and can be confused. Sand reflects visible sunlight well, making difficult the detection of smaller-sized clouds over deserts. The ability of infrared sensors to discriminate between clouds and cloudfree regions depends on the difference between the cloudtop temperature and the underlying surface skin temperature. Infrared cloud detection is difficult where thermal contrast between cloud and background are weak; this is most common for low stratus and cumulus clouds over the ocean or at night.

Many of these limitations in cloud imagery analysis can be overcome using additional channels of multispectral meteorological sensor data. Radiometers for visible, near-infrared, infrared, and microwave channels exist or are being developed for the primary sensors of the Defense Meteorological Satellite Program (DMSP) and National Oceanographic and Atmospheric Administration (NOAA) spacecraft. When used together, these channels discriminate between low clouds and clear regions, snow and clouds, and precipitating from non-precipitating clouds. This paper describes one method which simultaneously combines up to three "black-and-white" meteorological images into a color image product. It is found that such color imagery is more easily and confidently interpreted than is single-channel black-and-white imagery.

Color-composite image products are not new. They have been generated routinely using Landsat Multispectral Scanner (MSS) imagery data; these data reveal valuable information on geological, agricultural, and urban features (Colwell, 1983), but not very much information on clouds. The Space Department of the Royal Aircraft Establishment, Farnborough, England generates color image products using the infrared channels from the NOAA AVHRR (Bunting, personal communication, 1987).

At the Air Force Geophysics Laboratory (AFGL) this technique has been refined and applied to incorporate other meteorological image data. Such data include the "split-visible" channels of the NOAA Advanced Very High Resolution Radiometer (NOAA AVHRR); the visible, near-infrared, infrared, and low-light level (PMT) channels of the DMSP Operational Linescan System (OLS); and the GOES VISSR Atmospheric Sounder (VAS) infrared channels with either the 3.7μm window channel or the 6.7μm water vapor channel. In addition, color image products have been generated using data from the Nimbus-7 Scanning Multifrequency Microwave Radiometer (SMMR) and the DMSP SSM/I Microwave/Imager. A brief description follows of some of these sensors. The technique used to generate color image products is described in following sections, and some image examples are presented along with a discussion of their applications.

2. Meteorological Satellites and Sensors

The AVHRR, the primary sensor of NOAA polar orbiters, is a scanning radiometer that simultaneously senses in the five channels listed in Table 1. Channels 1 and 2 sense reflected sunlight and are used to detect cloud and snow cover, sea ice, and even volcanic dust plumes. The channel 3 sensor measures energy in the 3.7μm wavelength region. At nighttime the channel 3 sensor measures emitted thermal radiation with characteristics that are nearly similar to the longer-wavelength 10-12μm infrared channels. However during the daytime, the channel 3 sensor measures not only emitted thermal but also reflected solar energy. Reflected sunlight is usually a significant part of daytime channel 3 measurements (Smith and Rao, 1972) making channel 3 daytime imagery interpretations more difficult. Channel 4 senses emitted thermal energy, and is used for the thermal mapping of clouds and the earth's surface both day and night. Channel 5 also senses emitted thermal energy and has similar characteristics as channel 4, except that channel 5 radiation is more sensitive to atmospheric water vapor attenuation. When measured in moist atmospheres, channel 5 brightness temperatures are as much as 3% lower than their corresponding channel 4 temperatures.

The Nimbus-7 SMMR is a conically scanning radiometer that simultaneously senses emitted microwave radiation in the five channels listed in Table 2. Nimbus-7 SMMR measurements are used to determine geophysical parameters such as ice age, concentration, and edges; snow edges; cloud liquid water; precipitation rates; and soil moisture.

The OLS, the primary meteorological sensor of the DMSP, is a scanning radiometer that simultaneously senses reflected sunlight and emitted thermal energy in the two channels listed in Table 3. The visible channel is used to detect clouds and smokes over land; the infrared channel is used to map thermal radiation emitted by clouds, the earth's surface, and oceans both day and night.

A new set of channels is being proposed for development on future DMSP OLS primary sensors. They are listed in Table 4. The "split-visible" sensors measure reflected solar radiation in the visible and near-infrared wavelength regions. The Photomultiplier Tube (PMT) is a low-light-level nighttime visible sensor which

NOAA AVHRR Channels	
Channel	*Spectral Band*
1	0 55-0 70μm
2	0 72-1 1μm
3	3 5-3 9μm
4	10 3-11 3μm
5	11 5-12 5μm

Table 1. Spectral intervals for the NOAA AVHRR channels.

Five-channel Nimbus-7 SMMR				
Channel 1	*Channel 2*	*Channel 3*	*Channel 4*	*Channel 5*
6 6 GHz V	10 7 GHz V	18 GHz V	21 GHz V	37 GHz V
6 6 GHz H	10 7 GHz H	18 GHz H	21 GHz H	37 GHz H

Table 2. Spectral intervals for the five Nimbus-7 SMMR channels. "V" denotes vertical polarization; "H" denotes horizontal.

DMSP OLS Channels	
Channel	*Spectral Band*
Visible	0 4-1 1μm
PMT	0.5-0 9μm
Infrared	10-13μm

Table 3. Spectral intervals for the DMSP OLS channels.

DMSP SSM/I Channels	
Frequency	*Polarization*
19.35 GHz	Vertical, Horizontal
22.2 GHz	Vertical
37 GHz	Vertical, Horizontal
85.5 GHz	Vertical, Horizontal

Table 5. Spectral interva'ls for the DMSP SSM/I channels.

Potential Multispectral DMSP OLS Channels	
Channel	*Spectral Band*
Visible "Blue"	0 5-0 7μm
Near-infrared "Red"	0 7-1 1μm
Broadband Visible	0 5-1 1μm
PMT	0 5-0 9μm
Snow/Cloud	1 5-1 6μm
Low Cloud	3 5-3 9μm
Thermal "Blue"	10 3-11 4μm
Thermal "Red"	11 4-12 5μm
Broadband Infrared	10 3-12 5μm

Table 4. Spectral intervals for the Multispectral DMSP OLS channels.

measures reflected moonlight, and is also sensitive to city lights. The "snow/cloud" sensor measures reflected solar energy at 1.6μm during daytime only; 1.6μm emissions from terrestrial surfaces are too weak to be detected, so that no useful nighttime data is obtainable. The "low cloud sensor" measures thermal emission and reflected sunlight during daytime and thermal emission at night, just as the AVHRR channel 3 sensor. The "split infrared" window measures emitted thermal energy at the longer infrared wavelengths. It is possible that these sensors will fly on DMSP by the mid 1990's; some of these channels exist or are also scheduled for the NOAA-K, -L, and -M polar orbiters in the early 1990's.

A new microwave sensor was launched on the operational DMSP-F8 spacecraft in mid-1987. This sensor, called the Special Sensor Microwave/Imager (SSM/I), was developed for DMSP as an all-weather meteorological and oceanographic sensor. It is a passive, conically-scanning radiometer that measures microwave energy at the 4 frequencies listed in Table 5 (Felde et al., 1987). The SSM/I shows promise in providing estimates of ice concentration, snow cover, rain rates, and cloud liquid water content. The DMSP OLS provides high-resolution visible and infrared data coincident in space and time with the SSM/I data, and the DMSP Microwave Temperature Sounder (SSM/T) provides coincident atmospheric temperature profile data.

3. Generating and Interpreting Color-Composite Meteorological Satellite Images

Multispectral data is often displayed as black-and-white images, one for each channel. It can be cumbersome to scan back-and-forth among these images in order to extract all the available information each has to offer. The following sections describe how coincident multispectral images can be combined into one color-composite image product that better reveals all the unique information the original images contain. The next section briefly describes the image processing capabilities AFGL has, followed by some multispectral color-composite examples.

3.1 *Image Processor Capability*

The AFGL Interactive Meteorological System (AIMS) uses two ADAGE image processors; each is a full-color system that receives input from red, green, and blue "color guns" in order to display an image on a color monitor. Each processor contains 4 Mbytes of memory, enough to display four 512 × 512 color images, with 32 bits available for each pixel within the image. The 32 bits are partitioned into 4 8-bit parts; one provides digital input to the red gun, one to the green, and one to the blue. The remaining part is used for graphic overlays

such as map outlines and surface weather observations. The 512 × 512 × 8 bits that drive the red gun are collectively referred to as the "red image plane", and similarly for the green, blue, and overlay planes. The processor can display the image planes simultaneously; the result is a "color-composite" image. For more details on the ADAGE image processors, please refer to the paper by Kleespies that is in these proceedings.

3.2 *Color-composite Infrared Imagery*

At night, the thermal channels of the NOAA AVHRR measure upwelling thermal radiances in three spectral bands. These radiances can be converted to equivalent brightness temperatures using the Planck blackbody relation; a grayshade image may then be constructed in which the highest temperatures (warmest bodies) are represented by the darkest grayshades, and the lowest temperatures (coldest bodies) are represented by the brightest grayshades. Clouds appear bright (since they are colder) and cloudfree areas appear dark (since they are warmer), much as they would appear in a "visible" grayshade image constructed from reflected solar radiance measurements. Figures 1, 2, and 3 show examples of black-and-white images constructed from channels 3, 4, and 5 of the NOAA AVHRR. They are for the southeastern United States at ~0300 Local Time on 11 June 1982.

A color image can be constructed by placing the 3.7μm channel 3 grayshade image in the red plane, which in turn drives the red gun; in a similar fashion the 10.7μm channel 4 and 11.8μm channel 5 grayshade images are used to drive the green and the blue guns, respectively. Figure 4 contains the "redshade" image generated by placing Figure 1 in the red plane; Figures 5 and 6 show the corresponding "greenshade" and "blueshade" images for Figures 2 and 3, respectively. The image processor then combines these three gun inputs and displays their combination as a color image. Figure 7 shows the color image generated by combining the images in Figures 4-6. As will be discussed, combining the three images this way improves their interpretability.

Consider some pixel within the color-composite image of Figure 7. If for that pixel the inputs from the red, green, and blue guns are the same, then the equal color contributions in combination with one another will yield a shade of gray for that pixel. However if among the three guns there are differences in their intensities, then their combination will not yield a shade of gray but rather a color that is the result of unequal contributions from the red, green, and blue guns. The colors in Figure 7 are thus indicative of differences among the brightness temperatures of the three IR channels for a given pixel, since the color-gun inputs are the infrared black-and-white grayshades (Figures 1-3) that are themselves proportional to brightness temperature.

These differences in brightness temperature among the 3 channels are primarily due to differences in the radiative properties of clouds and the earth's surface at 3.7, 10.7, and 11.8μm, with lesser effects due to atmospheric attenuation by water vapor. Since the emissivities, reflectivities, and transmissivities of most

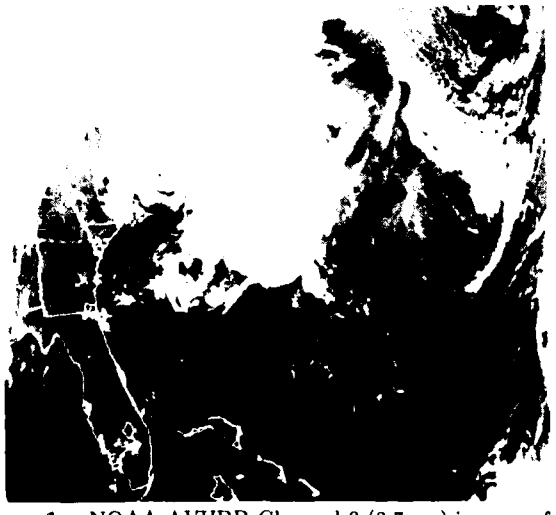

Figure 1. NOAA AVHRR Channel 3 (3.7μm) imagery for 11 June 1982 at ~0300 Local Time over the southeastern United States. The fog contrasts well with the adjacent cloudfree land (feature A).

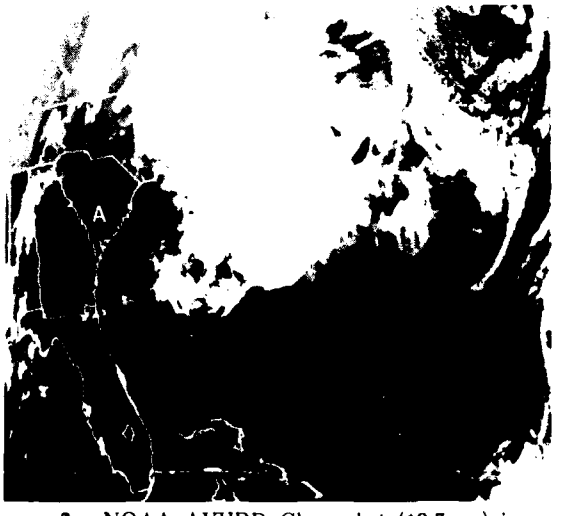

Figure 2. NOAA AVHRR Channel 4 (10.7μm) imagery for 11 June 1982 at ~0300 Local Time over the southeastern United States. The fog does not contrast well with the adjacent cloudfree land (feature A).

terrestrial surfaces change between 3.7 and 10-12μm, the measured brightness temperatures of those surfaces will also change (d'Entremont, 1986). The colors in infrared color composites (such as Figure 7) are generally characteristic of a particular cloud or underlying surface feature. Several of these features are now discussed.

Cloudfree Land and Water

In Figure 7 there is an excellent land/sea demarkation between the coasts of Florida and Georgia and the Atlantic Ocean. Open, cloudfree ocean is equally warm in all three channels and appears black. The brownish appearance of the cloudfree land is indicative of its emissivity differences. At the channel 3 wavelengths, most land surfaces have emissivities of ~0.9, while at channels 4 and 5 wavelengths they are ~1.0 (Colwell, 1983). In turn, channel 3 land brightness temperatures are 2-3 K lower than they are for channels 4 and 5 for the cloudfree land areas of western South Carolina and most of Georgia and Florida. Since the channel 3 brightness temperature is lower, the contribution to the pixel color from the red gun is stronger than that of both the green and blue guns. When combined, the stronger red contribution results in a pixel more brownish (i.e., more red) in appearance.

Low Clouds and Fog

One of the most significant problems facing nighttime cloud analysis using infrared satellite data is in detecting low clouds and fogs. Since such clouds lie close to the ground, they have temperatures that are close to the ground temperature; thus their temperature difference is not large enough to confidently discriminate them from each other. As a result low clouds are frequently mistaken for cloudfree land or ocean, and vice versa, in 10-12μm infrared black-and-white imagery.

The use of nighttime AVHRR channel 3 low cloud data helps to alleviate this problem. Fog and low clouds are often composed of water droplets; at 3.7μm wavelengths water droplet clouds have emissivities ranging from 0.35-0.90, depending on droplet sizes and total cloud optical depth (Hunt, 1972). Most land surfaces have emissivities of ~0.9 (Colwell, 1983). Thus the measured channel 3 brightness temperatures of typical fogs and low clouds are lower than they are for land; AVHRR nighttime imagery has shown this difference can be up to 5 K and more. Such temperature differences allow these clouds to contrast well with adjacent cloudfree surfaces in channel 3 imagery, leading to a confident discrimination between the two features. Feature "A" in Figure 1 shows such an example; this fog in eastern South Carolina (which was reported by many surface observers at the time of the image) contrasts well with the adjacent cloudfree land just to the west. Note that this contrast is much better than it is in the coincident longer-wavelength channel 4 imagery in Figure 2.

Figure 3. NOAA AVHRR Channel 5 (11.8μm) imagery for 11 June 1982 at ~0300 Local Time over the southeastern United States. The fog does not contrast well with the adjacent cloudfree land (feature **A**).

In the multispectral color-composite image of Figure 7, low clouds and fog are reddish in appearance due to its emissivity differences from 3.7 to 10-12μm. As previously stated, 3.7μm emissivities range from 0.35-0.90; at 10-12μm wavelengths, the emissivities for such clouds are nearly unity (Hunt, 1972). This makes AVHRR channel 3 low cloud/fog brightness temperatures lower than they are for channels 4 and 5; channel 3 brightness temperatures are 4-7 K lower for the low clouds and fog in eastern South Carolina. Since the channel 3 brightness temperature is lower, the channel 3 grayshade is higher and hence the contribution to the pixel color from the red gun is stronger than that of both the blue and the green guns. When combined, the stronger red contribution results in a more reddish pixel.

How red a low cloud pixel appears depends on the cloud's emissivity at channel 3 wavelengths. If the channel 3 emissivity is low, the multispectral pixel color is a deeper red; if the emissivity is higher (but not unity), the multispectral pixel color is pinkish. For

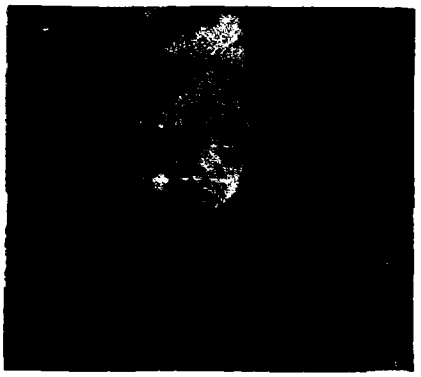

Figure 4.

Figure 5.

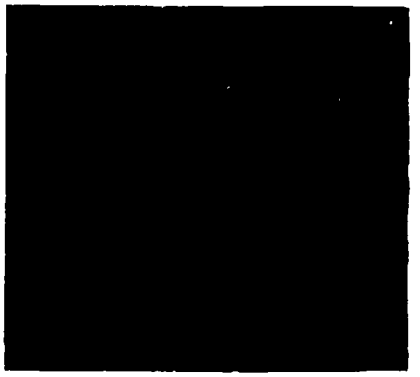

Figure 6.

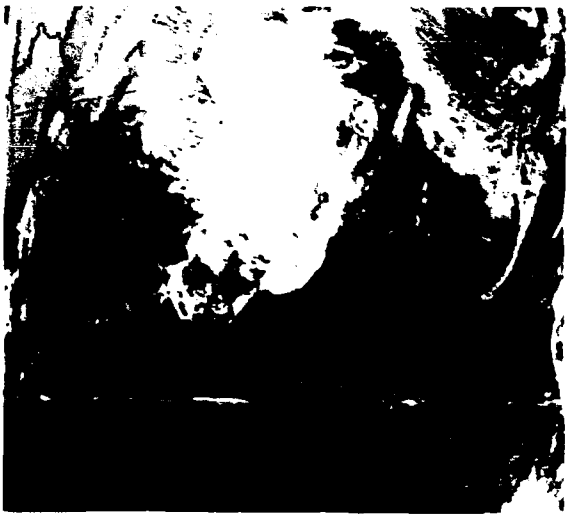

Figure 7.

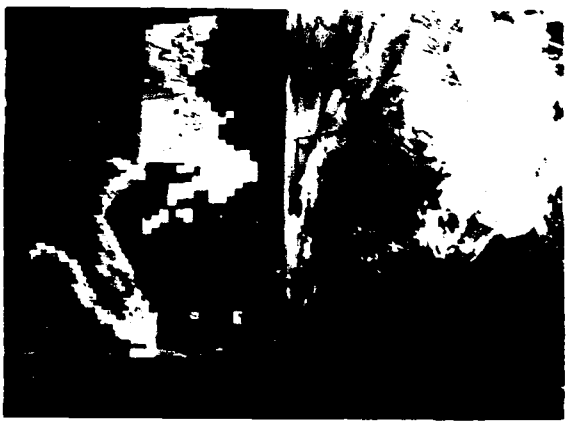

Figure 8.

Figure 11.

Figure 13.

Figure Captions for Color Images
Figure 4. The image obtained when placing Figure 1 into the "red plane" of the ADAGE image processor.
Figure 5. The image obtained when placing Figure 2 into the "green plane" of the ADAGE image processor.
Figure 6. The image obtained when placing Figure 3 into the "blue plane" of the ADAGE image processor.
Figure 7. Infrared color-composite image of the southeastern United States generated by simultaneously displaying the images in Figures 4-6.
Figure 8. Color-composite SMMR 37 GHz microwave image (left) of the southeastern United States for 11 June 1982 at midnight Local Time, and the nearly coincident AVHRR infrared image (right) taken from Figure 7.
Figure 11. "Split-visible" color-composite image of the northeastern Unites States and southeastern Canada generated by simultaneously displaying the images in Figures 9 and 10.
Figure 13. Color-composite visible/snow-cloud image of the eastern United States and southeastern Canada generated by simultaneously displaying the visible and snow-cloud images in Figure 12.

example, the stratocumulus in the upper right quadrant of Figure 7 appears pink, because stratocumulus emissivities are larger than the fog emissivities. In turn the stratocumulus channel 3 brightness temperatures are lower than the channel 4 brightness temperatures by 3-4 K, in comparison to 4-7 K for the fog.

In comparison to the blue and green guns, the red gun's contribution is stronger for fog and low clouds than it is for cloudfree land. This is because the *differences* between the channel 3 and channels 4 and 5 brightness temperatures for fog and low clouds are as much as double those for land. That is why fog and low clouds look redder than cloudfree land.

Cirrostratus and Cirrus

In Figure 7, thick cirrus and cirrostratus clouds in association with an area of thunderstorms can be seen offshore, east of the Carolinas and Virginia. These clouds appear grayish in Figure 7, indicative that their emissivity differences are not as great as for low clouds and cloudfree land. At Channel 3 wavelengths, emissivities for thick ice clouds approach unity, depending on the ice particle sizes and total cloud optical depths; emissivities at channels 4 and 5 wavelengths are nearly unity (Hunt, 1972). In turn, brightness temperatures from all three channels are similar. Thus the contributions from each of the three color guns are approximately equal. When combined, the result is a pixel that is grayish in appearance (no color dominates the pixel color).

There are thin cirrus clouds along the eastern edge and ahead of the thunderstorms and rain showers. The thin cirrus appears turquoise due to the mixture of sources (warm surface and cold cloud) within each cirrus pixel. Channel 3 is much more sensitive than channels 4 or 5 to warm scenes due to the stronger dependence of the Planck function on temperature at channel 3 wavelengths (Smith and Rao, 1972). Consequently the channel 3 brightness temperatures are higher since proportionally more 3.7μm radiance is contributed to the total upwelling radiance by the warmer surfaces beneath the cirrus. AVHRR nighttime measurements have indicated that for thin cirrus, channel 3 brightness temperatures can be up to 15 K higher than channels 4 and 5 brightness temperatures. Since the channel 3 brightness temperature is higher, the contribution to the pixel color from the red gun is weaker than that of both the green and blue guns. When combined the stronger green and blue contributions result in a pixel that appears more greenish-blue, or turquoise.

3.3 *Color-composite Microwave Imagery*

Figure 8 contains color images of the southeastern United States; on the left is a SMMR microwave image, and on the right for comparison is a subimage of the AVHRR infrared image in Figure 7. The infrared color image is valid for 11 June 1982 at ~0300 Local Time. The microwave image contains data from two Nimbus orbits. The eastern half is for 11 June 1982 at midnight Local Time, while the western half is from a subsequent Nimbus orbit nearly 12 hours later at noon Local Time. The time between the morning SMMR image and the AVHRR image is almost 3 hours. Although this difference is too large for direct comparison between the images on a pixel-by-pixel basis, the times are still close enough to allow for some useful, general comparisons of the overall image features.

The microwave color image was generated by simultaneously combining imagery from the 37 GHz vertical and horizontal polarization channels of the SMMR. The 37 GHz measured brightness temperatures are converted to a grayshade image in which the highest temperatures are represented by the darkest grayshades, and the lowest temperatures are represented by the brightest grayshades. The 37 GHz horizontal grayshade image is then placed into both the red and blue ADAGE image processor planes, which drive the red and blue guns, respectively; similarly the 37 GHz vertical grayshade image is used to drive the green gun. The image processor then combines the three gun inputs and displays this combination as a color image, shown on the left side of Figure 8. Several interesting features contained in this microwave composite are now discussed.

Coastlines

The land/sea demarkation is pronounced. Land contrasts well with the ocean since the ocean emits poorly at 37 GHz and therefore appears significantly colder than the adjacent land. For the morning SMMR orbit the 37 GHz vertical brightness temperatures are 30-40 K lower for the ocean than for the land; for the 37 GHz horizontal they are 60-75 K lower. All pixels with brightness temperatures 190 K or less have been enhanced blue, so that the ocean appears blue in Figure 8. Notice that the coastline is well defined even in the presence of the clouds over the eastern Carolinas and Virginia. This is because 37 GHz microwave energy emitted from the underlying surface can penetrate clouds with low liquid water content.

Precipitation

Microwave radiation at 37 GHz frequencies is relatively insensitive to clouds with low liquid water content, but not to precipitating clouds and clouds with high liquid water content. Clouds that contain heavy precipitation will prevent microwave sensors from seeing all the way to the earth's surface. The grayish-purple area southeast of the North Carolina coast indicates the presence of precipitating clouds and clouds with high liquid water content. This area is associated with the thicker white clouds seen in the corresponding infrared image (right side of Figure 8). The reason that the precipitation contrasts well with the ocean surface is that rain emits 37 GHz energy better. The result is that the rain areas appear significantly warmer than the ocean in the microwave imagery. The 37 GHz vertical rain brightness temperatures are 220-230 K, compared to 190 K and lower for the ocean. The 37 GHz horizontal rain brightness temperatures are 210-220 K, compared to 145 K and lower for the ocean. The grayish-purple appearance of the precipitation is indicative of small temperature differences between the vertical and horizontal polarizations. Since the horizontal temperatures are ~10 K lower than the vertical temperatures, the contribution to the pixel color is stronger from the red and blue guns. When combined, the stronger red and blue contributions result in a pixel that appears more reddish-blue, or purple. On the precipitation edges these differences are not large, so that the contribution to each of the color guns is nearly equal; this results in a grayish pixel.

At 37 GHz the brightness temperature difference is not as large between land and precipitation as it is between the ocean and precipitation. Land can be as good an emitter as rain of 37 GHz microwave energy, depending on the intensity and size of the raindrops. Thus in Figure 8, the contrast is not good between the precipitation and adjacent precipitation-free land areas.

3.4 *Color-composite "Split-Visible" Imagery*

Visible data are useful for cloud detection since clouds usually reflect sunlight more strongly than most backgrounds. The AVHRR has sensors which measure reflected sunlight in the 0.63μm visible and 0.86μm near-infrared spectral bands (channels 1 and 2, respectively). Water reflects incoming solar radiance poorly in both channels 1 and 2, and appears dark in the imagery. Clouds reflect sunlight equally well in both channels, and appear bright in the imagery. However, land backgrounds reflect visible light poorly when compared with the near-infrared. Surface albedoes for cloudfree land can be as much as 40% lower for channel 1 wavelengths than they are for channel 2 (Bowker et al., 1985; Colwell, 1983). Thus land backgrounds that appear bright in the channel 2 imagery appear dark in the channel 1 imagery. Clouds are detected more easily in channel 1 imagery because the difference between most backgrounds and clouds is greater than it is for channel 2 imagery.

Figure 9. NOAA AVHRR Channel 1 (0.63μm) visible imagery of the northeastern United States and southeastern Canada for 11 June 1982 at ~1500 Local Time. Coastlines do not show up well in this image, but small-scale cumulus contrast well with cloudfree land.

Figure 10. NOAA AVHRR Channel 2 (0.86μm) near-infrared imagery of the northeastern United States and southeastern Canada for 11 June 1982 at ~1500 Local Time. Coastlines show up well in this image, but small-scale cumulus often do not contrast well with cloudfree land.

Figures 9 and 10 illustrate the differences between visible and near-infrared imagery from the AVHRR channels 1 and 2. The images are for ~1500 Local Time on 11 June 1982 for the northeastern United States, southeastern Canada, and the Great Lakes. Bright tones indicate surfaces that reflect sunlight well, while dark tones denote surfaces that reflect sunlight poorly. Cape Cod and the New England coast contrast well with the ocean in the channel 2 image (Figure 10) while not nearly as well in channel 1 (Figure 9). The Great Lakes also contrast better with the adjacent land regions in the channel 2 image. In general, land/ocean boundaries are well-defined in the near-infrared imagery. However the cumulus clouds in the center section of the images (south of the Great Lakes and west of the frontal band over the eastern seaboard) are easier to detect in the channel 1 imagery. Channel 1 imagery is best for cloud detection but is not always helpful in locating land/ocean boundaries; channel 2 imagery is helpful in locating coastlines but clouds can be more easily confused with cloudfree backgrounds. A method is now described to combine the best characteristics of both images into a color-composite image in which coastlines, clouds, and clear areas are all easily detectable.

A color image can be constructed by placing the channel 1 black-and-white image (Figure 9) in both the red and the blue planes, which in turn drive the red and the blue guns; in a similar fashion the Channel 2 image (Figure 10) drives the green gun. The image processor then combines the three gun inputs and displays this combination as the color image shown in Figure 11. Combining the two black-and-white images this way brings the best characteristics of each into one color image product. The colors of Figure 11 are explained in the following paragraph.

There is an excellent cloud/no cloud demarkation throughout this image. Clouds are equally bright in each of the two channels and thus appear bright gray and white in their color composite. The greenish appearance of the cloudfree land is indicative of its reflectivity differences from channel 1 to channel 2 wavelengths. Most land surfaces have reflectivities at the channel 1 (0.63μm) wavelengths that are lower than they are at the Channel 2 (0.86μm) wavelengths (Colwell, 1983). In turn, channel 1 land albedoes are lower than they are for channel 2; channel 1 albedoes can be as much as 40% lower for cloudfree land (Bowker et al., 1985). Since the channel 2 land albedo is higher, the contribution to the overall pixel color from the green gun is stronger than that of both the red and blue guns. When combined, the stronger green contribution results in a pixel more green in appearance. There is also an excellent coastline definition throughout the image. Water, which reflects both visible and near-infrared light poorly, appears black in each of the two channels and thus appears dark in their color composite, contrasting well with the green land surfaces.

3.5 *Color-composite "Visible/snow-cloud" Imagery*

Improved cloud sensing has been demonstrated using data from an experimental 1.6μm near-infrared sensor flown on the DMSP F-4 satellite in 1979 (Bunting and d'Entremont, 1982). This is called the SSC or "snow/cloud discriminator" channel because snow backgrounds contrast well with low clouds in SSC imagery, unlike they do in visible channels. This is because snow absorbs 1.6μm energy well, while water droplet clouds reflect it much as they do at visible wavelengths. In SSC imagery the contrast between clouds and snow is good. At wavelengths of 1.6μm, snow reflects sunlight poorly while cloud liquid water droplets reflect it efficiently (Bunting and d'Entremont, 1982). An example is shown in Figure 12; this image stretches from the Carolinas northward to Quebec. The upper left part of each image strip contains clear skies and snow cover. The snow is bright in the 0.4-1.1μm visible imagery (because it reflects well) but dark in the 1.6μm near-infrared imagery (because it reflects poorly). In the upper right corner of each strip there are water droplet clouds. These clouds appear bright in the 1.6μm imagery, contrasting well with the adjacent dark snow cover. This contrast is not nearly as distinct in the visible imagery since both the clouds and the snow reflect visible sunlight well.

A color image can be constructed by placing the OLS visible-channel grayshade image (left strip in Figure 12) in the red and the blue planes, which in turn drive the red and the blue guns; in a similar fashion the SSC image (center strip in Figure 12) is used to drive the green gun. The image processor then combines the three gun inputs and displays their combination as a color image. Figure 13 shows an example of a visible/snow-cloud color image. Again, the differences between features in both the visible and the snow-cloud image are enhanced with colors that are indicative of differences between the albedoes of the OLS visible (0.4-1.1μm) and Snow-cloud (1.6μm) channels for a given pixel. These differences are due to differences in the reflective properties of clouds, snow, and the earth's surface at visible and near-infrared wavelengths.

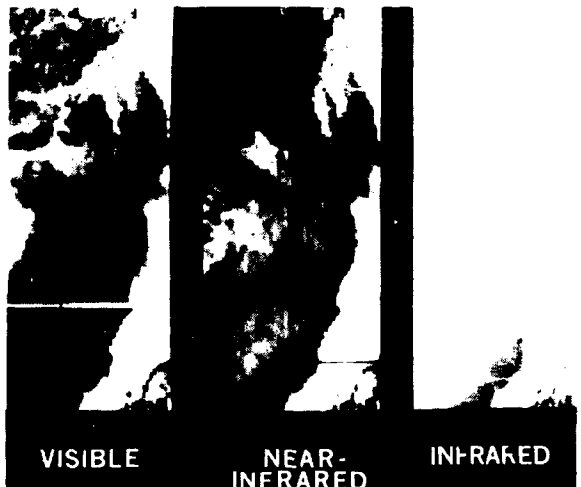

Figure 12. DMSP OLS visible (0.4-1.1μm, left strip), SSC (1.6μm, center strip), and OLS infrared (8-13μm, right strip) imagery for 17 December 1979 over the eastern United States and southeastern Canada. Bright tones denote highly reflective surfaces and dark tones denote poorly reflective surfaces in both the visible and SSC images. Bright tones denote cold surfaces and dark tones denote warm surfaces in the infrared image. Snow located in the upper left corner of each image appears dark the SSC imagery because it reflects 1.6μm radiation poorly.

There is an excellent snow/cloud/cloudfree demarkation throughout this image. Clouds are equally bright in each of the two channels and thus appear bright in their color composite. The greenish appearance of the cloudfree land is indicative of its reflectivity differences. Most land surfaces have reflectivities at the near-infrared wavelengths (1.6μm) that are higher than they are at the visible wavelengths (0.4-1.1μm). In turn, SSC land albedoes are higher than they are for visible channels (Bowker et al., 1985). Since the SSC land albedo is higher, the contribution to the overall pixel color from the green gun is stronger than that of both the red and blue guns. When combined, the stronger green contribution results in a pixel more green in appearance. Green pixels are thus indicative of cloudfree land surfaces. Cloudfree ocean surfaces are dark in both visible and SSC imagery, so that their combination appears dark in their color composite.

As previously discussed, snow cover has reflectances that are lower at near-infrared wavelengths (1.6μm) than they are at the visible wavelengths (0.4-1.1μm) (Bunting and d'Entremont, 1982). In turn, SSC snow albedoes are lower than they are for visible channels. Since the SSC snow albedo is lower, the contribution to the overall pixel color from the green gun is weaker than that of both the red and blue guns. When combined, the stronger red and blue contributions result in a pixel more purple in appearance. Purple pixels are thus indicative of cloudfree, snow-covered surfaces.

Ice particle clouds also reflect sunlight poorly at 1.6μm, but usually not as poorly as snow cover (Bunting

and d'Entremont, 1982). The differences are large enough so that ice clouds also contrast well with water droplet clouds in 1.6μm imagery. Hence the phase of clouds can also be determined using snow/cloud color composites; ice particle clouds such as cirrus, cirrostratus, and cumulonimbus appear light purple in the visible/snow-cloud color composite as well.

4. Summary and Discussion

A fast, effective method has been described that simultaneously combines multichannel satellite data into a color image product. The method generates a color-composite image product that concisely combines the most desirable characteristics of images from several spectral channels into one image. Such color composites clearly reveal features of meteorological interest to the user.

Discrimination between low clouds/fogs and cloudfree land/oceans, along with improved detection of thin cirrus, can be performed more confidently when using multispectral infrared color-composite imagery. Existing infrared and microwave imagery indicate that discrimination between opaque cirrus and nimbostratus can be performed successfully over oceans. The presence of snow cover and ice can also be detected more confidently using visible and near-infrared data in conjunction with one another.

Availability of upcoming DMSP and NOAA multispectral imagery along with DMSP microwave imagery will make it possible to generate such color products in increasing amounts. The use of these meteorological channels in conjunction with one another can greatly enhance the quality of cloud image interpretations that use only visible and/or infrared data as a primary source of information. The quality can be enhanced of cloud analyses and subjective imagery interpretations which use only infrared black-and-white imagery as a primary source of information. Studies are ongoing at AFGL to make more efficient use of coincident multispectral visible, near-infrared, infrared, and microwave data to improve Air Force real-time operational global analyses of clouds and the earth's surface conditions.

5. Acknowledgements

We wish to extend our thanks to members of AFGL's Satellite Meteorology Branch who have been working over the past year on developing the AFGL Interactive Meteorological System (AIMS) which generates the artificial color imagery; Thomas J. Kleespies for his efforts in documenting the ADAGE image processing utility software; and to Gerald W. Felde, Gary B. Gustafson, Kenneth R. Hardy, Charles F. Ivaldi, and D. Keith Roberts for their continuing work in upgrading AIMS hardware and software capabilities. We also wish to thank Lee Stevens of the AFGL Photo Lab who was responsible for photographing the images presented in this paper.

6. Bibliography

Bowker, David E., Richard E. Davis, David L. Myrick, Kathryn Stacy, and William T. Jones, 1985: "Spectral Reflectances of Natural Targets for Use in Remote Sensing Studies." NASA Reference Publication 1139, June 1985, 181 pp.

Bunting, J. T. and K. R. Hardy, 1984: "Cloud Identification and Characterization from Satellites." *Satellite Sensing of a Cloudy Atmosphere: Observing the Third Planet*, A. Henderson-Sellers, Ed., Taylor and Francis, London, 340 pp.

Bunting, J. T. and R. P. d'Entremont, 1982: Improved Cloud Detection Utilizing Defense Meteorological Satellite Program Near Infrared Measurements. Air Force Geophysics Laboratory Technical Report AFGL-TR-82-0027, National Technical Information Center Document ADA 118751.

Colwell, Robert N. (Ed.), 1983: *Manual of Remote Sensing, Volume I: Theory, Instruments, and Techniques*. Amer. Soc. of Photogrammetry, Falls Church, VA, 94-95.

d'Entremont, Robert P., 1986: Low- and Midlevel Cloud Analysis Using Nighttime Multispectral Imagery. *Journ. Clim. and Appl. Meteor.*, 25, 1853-1869.

Felde, Gerald W., J. T. Bunting, and K. R. Hardy, 1987: Atmospheric Remote Sensing in Arctic Regions. DoD Symposium and Workshop on Arctic and Arctic-Related Environmental Sciences, 27-30 January 1987, A. Deepak Publishing (Div. of Science and Technology Corp.), Hampton, VA.

Hunt, G. E., 1972: Radiative properties of terrestrial clouds at visible and infra-red thermal window wavelengths. *Quart. J. Roy. Meteor. Soc.*, 99, 346-359.

McClain, E. Paul, 1981: Multiple atmospheric-window techniques for satellite-derived sea surface temperatures. *Oceanography from Space*, Plenum Publ. Corp., 73-85.

Rowan, Lawrence C., P. H. Wetlaufer, F. H. Goetz, F. C. Billingsley and J. H. Stewart, 1974: "Discrimination of Rock Types and Detection of Hydrothermally Altered Areas in South-central Nevada by the Use of Computer-enhanced ERTS Images." Geological Survey Professional Paper 883, United States Government Printing Office, Washington, 35 pp.

Smith, W. L., and P. K. Rao, 1972: The Determination of Surface Temperature From Satellite 'Window' Radiation Measurements. *Temperature: Its Measurement and Control in Science and Industry*, 4, Symposium on Temperature, 1971, Washington, D.C.: Instr. Soc. of Amer., 2251-2257.